agriculture

MDPI

Article

Effects of Five–Year Inorganic and Organic Fertilization on Soil Phosphorus Availability and Phosphorus Resupply for Plant P Uptake during Maize Growth

Jingjing Zhang [1], Jiong Wen [2], Tuo Zhang [1], Yang Zhang [1,2], Zhi Peng [2], Chunchun Tang [2], Yanan Wang [1,2], Shiming Su [1,2], Nan Zhang [1] and Xibai Zeng [1,2,*]

[1] Key Laboratory of Agro–Environment, The Ministry of Agriculture of China, Institute of Environment and Sustainable Development in Agriculture, Chinese Academy of Agricultural Sciences, Beijing 100081, China
[2] Yueyang Agricultural Environment Scientific Experiment Station, Ministry of Agriculture, Yueyang 414000, China
* Correspondence: zengxibai@caas.cn

Abstract: A better understanding of the P dynamic resupply roles of fertilization from soil solids to solution is urgently required to optimize sustainable P fertilizer management practices for efficient supply. A five–year fertilization experiment was used to investigate the effects on soil P fractions and availability, the kinetic P resupply based on a novel simulation technique (Diffusive gradients in thin films (DGT) and DGT–induced fluxes in sediments and soils (DIFS)) and to identify dominant factors during the maize season under five treatments (no fertilizer (CK), chemical fertilizer (NPK), chemical fertilizer combined with bone meal fertilizer (NPKC), crop straw (NPKS) and bioorganic fertilizer (NPKM)). The results showed that the NPKC and NPKM treatments had higher enhancement effects on Olsen–P and organic P and inorganic Ca_2–P, Ca_8–P, Al–P and Fe–P at maize growth stages, and they buffered pH decrease to delay the substantial Fe–P and Al–P release until a late stage. Inorganic Ca_2–P, Ca_8–P, Al–P and Fe–P heavily effected the Olsen–P levels. The NPKS, NPKC and NPKM treatments yielded higher C_{DGT}–P levels and a stronger resupply capacity, reflected by higher R and C_E/C_{soln} and smaller T_c values. The simulation and path model results revealed that the maize plant P uptake was determined by soil P resupply and an inorganic P supply pool. They were positively dominated by soil organic matter (SOM). Our results suggested that organic fertilization, especially NPKC and NPKM treatments, provided greater enhancement effects on the P supply pool and P resupply for higher plant P uptake, identifying them as highly effective P management practices for developing sustainable agriculture.

Keywords: organic fertilizer; phosphorus; dynamic resupply; DGT and DIFS

check for updates

Citation: Zhang, J.; Wen, J.; Zhang, T.; Zhang, Y.; Peng, Z.; Tang, C.; Wang, Y.; Su, S.; Zhang, N.; Zeng, X. Effects of Five–Year Inorganic and Organic Fertilization on Soil Phosphorus Availability and Phosphorus Resupply for Plant P Uptake during Maize Growth. *Agriculture* **2023**, *13*, 858. https://doi.org/10.3390/agriculture13040858

Academic Editors: Arvind Kumar Shukla, Sanjib Kumar Behera, Salwinder Singh Dhaliwal and Mahesh Chand Meena

Received: 13 March 2023
Revised: 1 April 2023
Accepted: 3 April 2023
Published: 13 April 2023

1. Introduction

Phosphorus (P) adequate supply is necessary for food production in agricultural soils, especially in low–P soils [1,2]. The typical low–P soils widely distributed in subtropical areas in the south of China are also an important source of available land, but are characterized by low pH and high levels of Fe– and Al– (hydr–)oxides that lead to high P adsorption capacities [3]. P deficiency and low P availability are major constraints of crop production in the soils. Many organic fertilizers derived from manure, compost, plant or animal residues, acting as alternative fertilizers, have long been progressively plowed into soils, partly to recycle P resources and improve P bioavailability [4,5]. Simultaneously, when the soil is saturated to a point above the environmental threshold level of P, long–term organic fertilization increases the potential of P desorption to soil solution and losses [6,7]. Pradhan et al. [7] demonstrated that twelve–year manure substitution of mineral fertilizer resulted in excessive accumulation of total P and available P, posing a great risk of P loss from soil to aquatic ecosystem. The quality and quantity of organic fertilizers to improve the P supply for plants in high–P–adsorbing soils must be determined to develop efficient management actions in sustainable agriculture. Thus, it is crucial for P fertilizer management optimization to predict the P supply potential comprehensively and accurately.

Soil P fractions and P availability are often explored as potential supply pools to evaluate the potential of soil P supply for plants [8,9]. Available P can readily be released to support plant uptake, and reversibly adsorbed P on Fe– and Al– (hydro)oxides and Fe–, Al– and Ca– minerals and organic P forms in soils can be released by desorption, dissolution or mineralization as potential available pools [10]. Organic fertilizers, except as P sources, can also affect P fractions and availability by changing the physical, chemical and biological characteristics of the soil [11–13]. Zhang et al. [12] reported that the application of long–term manure and straw substitution increased soil rapidly and slowly available P fractions by regulating pH and phosphatase. Nobile et al. [11] reported that, after ten years of manure fertilization, the enhancement of soil organic matter (SOM) and pH decreased P adsorption and, thus, increased the available P in soils. The increase in SOM can also increase phosphatase activities to catalyze organic P mineralization [5]. A decrease in soil available P was also observed in crop straw applications with a high C/P ratio [14]. The magnitude and intensity of the impact on soil P availability exerted by organic fertilizers could present distinct discrepancies over time and among various fertilizer types. Jalali and Ranjbar [15] reported that organic additions made the rapid P release during the first four weeks of the incubation phase, and the poultry and sheep manure with higher P contents had a higher P release concentration relative to plant residues. Alamgir et al. [16] also found that low–P organic residues decreased soil labile inorganic P and increased microbial P, and they also had an earlier decrease of medium labile organic P than high–P organic residues. These changes of P pools in the soils were generally vital to the P supply for satisfying plant demands over different growth periods [17,18].

The amount of P loosely absorbed in soil (*Q*, P quantity), the concentration of P in the soil solution (*I*, P intensity) and the capacity to resist changes in solution P concentrations (PBC, P buffer capacity) jointly determine the P supply for plants [19,20]. Generally, plants continuously absorb soluble P from the soil solution, but the solution P concentration is usually much lower than the demand for optimal plant growth (0.2–0.8 mg $P \cdot L^{-1}$), especially in soils that highly adsorb P [21]. When solution P is depleted by plants, loosely absorbed P can be released, driving a new equilibrium between these fractions to achieve P resupply for plants [22]. Thus, the dynamic resupply from solids to solution is essential to explore the P supply for plant growth in red soil.

However, the conventional soil P tests for P availability are based on chemical extractants such as Olsen–P, Bray–P and $CaCl_2$–P, singly reflecting *Q* or *I* for the P supply [9]. The prediction results cannot be used to effectively predict the P supply potential, regardless of the dynamic resupply process and the limitations of the test methods [23,24]. Diffusive gradients in thin films (DGT) technology provides a new approach for dynamic detection of the labile P resupply [25]. The DGT device can concentrate the fluxes of soil liable P in situ as a sink by mirroring plant roots during deployment. Its measurement includes labile P in solution and labile P readily released from soil solids [26], integrally reflecting *Q*, *I* and PBC in soil. The DGT–induced fluxes in sediments and soils (DIFS) model was introduced to better interpret DGT measurements [27]. From DIFS simulations, the labile pool size and kinetic parameters of the soil P resupply can be obtained. The extensive usage of the DGT technique focused on a P availability assessment, and some work was also conducted to explore kinetic P resupply among various soils [25,28,29].

Organic fertilizer addition has great effects on phosphorus (P) availability for supply, but the role of kinetic P resupply in the improvement of organic fertilization on P supply for plants and the association with P supply pools in high–P adsorbing soils remain unclear. In this study, based on a five–year organic fertilizer experiment in typical subtropical low–P soil in southern China, samples analyses were carried out during the fifth maize–growing season to determine: (i) the influence of repeated organic fertilization on soil P fractions and P dynamic resupply; (ii) the relationship between P resupply and P supply pools; (iii) the contributions of fertilization treatments, critical factors, soil P supply pools and P resupply to maize P uptake. The goal of this study was to provide scientific fertilization practices for efficient P utilization and sustainable agricultural development.

2. Materials and Methods

2.1. Site Description and Fertilizer Treatments

This study was conducted at the Yueyang National Agricultural Experimental Station for Agricultural Environment in Hunan Province, China (29°23′ N, 113°06′ E) in 2016–2020. The region has a subtropical climate—the annual average temperature remained at 17.9 ± 0.2 °C and total precipitation was in the range of 1192–1909 mm in 2016–2020 (Figure 1). The field experiment performed a maize–rape rotation pattern and began with maize planting in May 2016. The soil type is Ferric Acrisol according to the FAO classification system [30]. The properties of the initial soil (0–20 cm) before the trial are listed in Table 1.

Table 1. Basic physicochemical properties of initial soil and three organic fertilizers.

Property	Initial Soil	Bone Meal Fertilizer	Rape Straw	Bioorganic Fertilizer
pH	5.46	7.96	–□	7.47
Total C ($g \cdot kg^{-1}$)	5.68	262	525	270
Total N ($g \cdot kg^{-1}$)	1.11	23.70	10.00	15.20
Total P ($g \cdot kg^{-1}$)	0.22	10.85	1.34	7.14
Total K ($g \cdot kg^{-1}$)	14.60	24.00	13.90	61.80
Total Fe ($g \cdot kg^{-1}$)	–	13.66	0.10	15.22
Total Al ($g \cdot kg^{-1}$)	–	20.21	0.11	28.84
Total Ca ($g \cdot kg^{-1}$)	–	73.76	0.83	60.56
Total Mg ($g \cdot kg^{-1}$)	–	18.29	0.77	15.78
Available N ($mg \cdot kg^{-1}$)	72.10	–	–	–
Available P ($mg \cdot kg^{-1}$)	3.84	–	–	–
Available K ($mg \cdot kg^{-1}$)	246.70	–	–	–

The details of the determination of the contents of above indicators are provided in the Supplementary Materials (SM2.1).

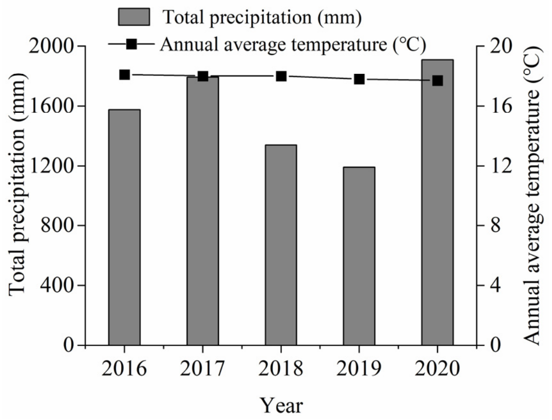

Figure 1. Annual average temperature (°C) and total precipitation (mm), 2016–2020 (Data from local meteorological station).

The following five treatments were selected: no fertilizer (CK); chemical fertilizer (NPK); chemical fertilizer and bone meal fertilizer (NPKC); chemical fertilizer and crop straw (NPKS); chemical fertilizer and bioorganic fertilizer (NPKM). All treatments were randomly arranged in 3 blocks (5 × 3 = 15 plots). Each plot was 8 m × 3.5 m. All fertilization treatments received equal amounts of 315 kg N ha^{-1}, 52.5 kg P ha^{-1} and 75 kg K ha^{-1} in the maize season. For the chemical fertilizer, N, P and K were provided by urea, superphosphate and potassium chloride, respectively. Bone meal fertilizer and bioorganic fertilizer with an effective viable count of B. subtilis $\geq$ 20 million colony–forming unit (CFU) g^{-1}, were purchased from Taigu Biotechnology Co. Ltd. (Hunan, China). Crop straw from the previous season was directly applied by mulching. Three organic fertilizers were consistently applied at a rate of 2250 $kg \cdot ha^{-1}$ in each crop season for sustainable and economic repeated application, according to the local application rates and the recommended low dose of organic fertilizers combined with chemical fertilizer, and their N, P and K contents were also derived from chemical fertilizer for equal nutrient levels. The above fertilizers were applied as base fertilizers at the beginning of each crop season. The specific properties of the organic fertilizers are also shown in Table 1.

2.2. Soil and Plant Sample Collection

Soil samples (0–20 cm) were collected from plant root zones at the seeding stage (21 May), flare–opening stage (16 June) and mature stage (1 August) during the maize growing season in 2020. The soil samples were partly air dried at room temperature, followed by sieving (2 and 0.145 mm) for further analysis, and residual sections were stored at 4 °C. The maize plants matched with the soil samples were also collected. Plant samples were dried at 75 °C to weigh their dry biomass and then crushed and sieved (0.145 mm).

2.3. Sample Analysis

Soil organic C was determined by the externally heated dichromate oxidation–colorimetric method [31], and was then converted into SOM contents by van Bemmelen factor 1.724 [32]. Soil pH (soil:water, 1:2.5) was determined by a Thunder pH meter (INESA, Shanghai, China). Amorphous Fe, Al (Fe_{ox} and Al_{ox}) and organic complexed Fe and Al (Fe_{PP} and Al_{PP}) were extracted with $(NH_4)_2C_2O_4$ (pH 4.2) and $Na_4P_2O_7$ (pH 8.5), respectively, and then determined by inductively coupled plasma–atomic emission spectrometry (ICP–AES) [33]. Soil organic P (OP) was obtained as the difference between combusted P and noncombusted P extracted with 0.5 M H_2SO_4 by the ignition method [34]. Olsen–P (available P) was extracted with 0.5 M $NaHCO_3$ (pH 8.5) [35]. Plant P content was measured by digestion with H_2SO_4–H_2O_2 [36] and then quantified by molybdate colorimetry at 800 nm using a spectrophotometer [37]. The P accumulation in the plant was calculated by multiplying plant P content by plant dry biomass.

The soil activities of four carbon–cycling enzymes (Sigma–Aldrich LLC, Shanghai, China), including α–1,4–glucosidase (αG, EC 3.2.1.20), β–1,4–glucosidase (βG, EC 3.2.1.21), β–1,4–xylosidase (βX, EC 3.2.1.37) and cellobiohydrolase (CBH, EC 3.2.1.91), were measured by fluorescence–based methods with 365 nm excitation and 450 nm emission filters using a microplate fluorometer (Scientific Fluoroskan Ascent FL, Thermo) [38]. Soil acid phosphatase (ACP) and alkaline phosphatase (ALP) were extracted using soil phosphatase kits (Solarbio, BC0140 and BC0280) and measured using a spectrophotometer at 405 nm (Acosta–Martínez and Tabatabai 2000).

2.4. Extraction of the Chemical Fractions of Inorganic P in Soils

Sequential inorganic P fractionation experiments were performed with the modified method described by Jiang and Gu [39]. The 1.00 g of soil was placed into a 100 mL tube and sequentially added the chemical extractants listed in Table 2 to the specifically obtained dicalcium phosphate (Ca_2–P), octocalcium phosphate (Ca_8–P), aluminum phosphate (Al–P), iron phosphate (Fe–P), occluded phosphorus (O–P) and apatite phosphate (Ca_{10}–P). The extracted P fractions were quantified by molybdate colorimetry at 800 nm using a spectrophotometer [37].

Table 2. Sequential inorganic P fractionation and corresponding chemical extractants.

P Fractions	Chemical Extractants
1. Ca_2–P	50 mL 0.25 M $NaHCO_3$, pH 7.5
2. Ca_8–P	50 mL 0.5 M CH_3COONH_4, pH 4.2
3. Al–P	50 mL 0.5 M NH_4F, pH 4.2
4. Fe–P	50 mL 0.1 M NaOH
5. O–P	40 mL 0.3 M $Na_3C_6H_5O_7$ + 1 g $Na_2S_2O_4$ + 10 mL NaOH
6. Ca_{10}–P	50 mL 0.25 M H_2SO_4

The extracted solution for O–P should be digested $H_2SO_4/HClO_4/HNO_3$ (1:2:7), before being quantified by molybdate colorimetry.

2.5. DGT Deployment, Theory Calculation and DIFS Model

In this study, DGT soil samplers (DGT Research Ltd., Lancaster, UK) equipped with a Zr–oxide binding layer were used for determining labile P. Detailed descriptions and information on the deployment of DGT devices can be found elsewhere [26,40]. Briefly, 30 g of air–dried soil was thoroughly mixed with water to obtain a smooth paste at a 100% water–holding capacity for 24 h at 25 °C. Then, the DGT sampler was gently inserted into the soil for 48 h at 25 °C. Then, the binding gel was removed from the DGT sampler and eluted in 1 mL of 1 M NaOH overnight at 25 °C. Part of the above soil paste centrifuged at 4000 $r \cdot min^{-1}$ for 30 min to obtain the soil solution. The P concentrations in both the eluent and the filtrate were quantified by the malachite green colorimetric method [41].

Based on Fick's first law of diffusion and DGT theory, the following parameters were calculated and DIFS simulations were conducted as described in previous reports [27,42,43]. First, the mass of P (M) accumulated in the binding gel was directly obtained as follows:

$$M = C\left(V_a + V_{gel}\right)/f_e \tag{1}$$

where C is the concentration of P in the elution of the binding gel, V_a and V_{gel} are the volumes of the acid eluent and the binding gel, respectively (V_a = 1 mL, V_{gel} = 0.15 mL) and f_e is the elution coefficient (f_e = 0.9). From M, the time–averaged concentration (C_{DGT}, $\mu g \cdot L^{-1}$) of P at the interface of the DGT device can be calculated based on Fick's first law of diffusion:

$$C_{DGT} = M\Delta g/DAT \tag{2}$$

where Δg is the thickness of the diffusive layer and protective layer (Δg = 0.78 mm), D is the diffusion coefficient for P in the diffusive gel (D = 6.05 × 10^{-6} cm^2/s, 25 °C), A is the surface area of the DGT sampling window (A = 2.54 cm^2) and T is the time of DGT deployment (T = 48 h).

The R value, reflecting the P resupply capability from the soil solids into solution, is the ratio of C_{DGT} to C_{soln}, as shown in Equation (3).

$$R = C_{DGT}/C_{soln} \tag{3}$$

C_{soln} is the initial concentration of P in the soil solution. R_{diff} is the critical R value where only porewater diffusion replenishes P depletion. R_{diff} is calculated using the DIFS model. From R_{diff}, C_{DGT} can be converted to C_E, the effective concentration, as follows Equation (4):

$$C_E = C_{DGT}/R_{diff} \tag{4}$$

C_E is defined as the solution concentration that can sustain the same mass accumulation in the device when the solution is undisturbed.

K_d is the solid–liquid partition coefficient of the labile P, which can be calculated as follows:

$$K_d = C_s/C_{soln} = k_1/(k_{-1}P_{c)} \tag{5}$$

where C_s is labile P adsorbed by the solid phase in soil. In this paper, C_s is referred to as Olsen–P. P_c is the soil particle concentration. k_1 and k_{-1} are the rate coefficients of adsorption and desorption, respectively, which can be determined using Equations (5) and (6), respectively:

$$T_c = 1/(k_1 + k_{-1}) \tag{6}$$

where T_c is the response time of the desorption process to depletion in the soil. T_c was derived from the 2D–DIFS model given R and K_d.

2.6. Statistical Analyses

The relevant samples data in this paper was collected form the 5th maize season. The seeding stage and flare–opening stage are known as the two crucial stages for maize P uptake for growth. A weak P uptake by maize occur at mature stage as the maize growth and grain formation is almost over. So, the study mainly focused on the soil available P supply and corresponding plant P uptake at the two key stages during the maize growth season. The significance of the difference ($p < 0.05$) between values was determined using Duncan's test in IBM SPSS 19.0 (SPSS, Inc., Chicago, IL, USA). One–way ANOVA was used to assess the difference between treatments and between growth stages, respectively. Redundancy analysis (RDA) was used to illustrate the relationships between the soil properties and P fractions in CANOCO 5.0 (Microcomputer Power, Inc., Ithaca, NY, USA). The partial least squares path model (PLS–PM) was employed to determine the relationships among the soil properties, enzyme activities, P fractions and plant P uptake using R (v.3.6.1) with the "plspm" package (1000 bootstraps). Pearson's method was used to evaluate the correlation between variables. In addition, "*" and "**" represent $p < 0.05$ and $p < 0.01$, respectively.

3. Results

3.1. Maize Plant P and Soil Labile P during the fifth Maize Season after Five–Year Fertilization

During the fifth maize season, plant P uptake was greatly influenced by fertilization ($p < 0.05$, Figure 2). Compared to NPK treatment, the NPKS, NPKC and NPKM treatments significantly increased plant P accumulation, and a significant difference was shown at the flare–opening stage, ranked as NPKM > NPKC > NPKS. For P contents, the NPKC and NPKM treatments significantly increased the contents at the seeding stage and flare–opening stage, while a similar advantage of the NPKS treatment occurred at the flare–opening stage.

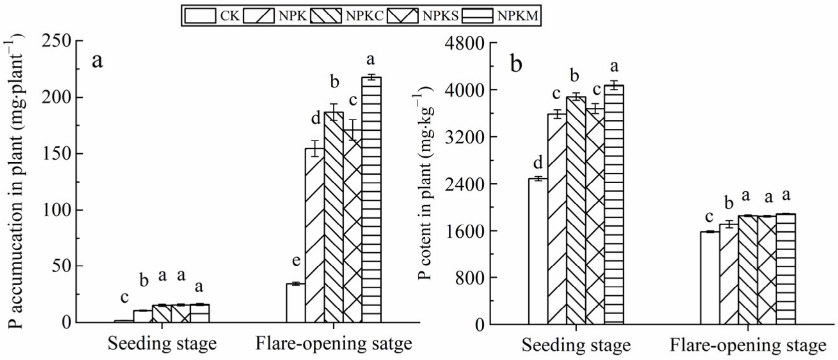

Figure 2. Effects of five years of fertilizer application on plant P accumulation (**a**) and plant P content (**b**). The different lowercase letters above the bars at the same stage indicate $p < 0.05$. CK: no fertilizer; NPK: chemical fertilizer; NPKC: chemical fertilizer and bone meal fertilizer; chemical fertilizer and crop straw NPKS; chemical fertilizer and bioorganic fertilizer NPKM.

Additionally, compared to NPK treatment, the NPKC and NPKM treatments had significantly higher Olsen–P and C_{DGT}–P, while the NPKS treatment scarcely increased Olsen–P but enhanced C_{DGT}–P at the seeding stage and flare–opening stage (Figure 3).

The highest C_{DGT}–P was always observed in the NPKM treatment (Figure 3). The Pearson coefficients showed that Olsen–P had strong correlations with the plant P content at the seeding stage ($R^2 = 0.713$, $p < 0.01$, Table 3). Indeed, C_{DGT}–P had a better correlation with the maize plant P uptake than Olsen–P, as reflected by the higher correlation coefficients ($0.666 < R^2 < 0.960$, $p < 0.05$, Table 3).

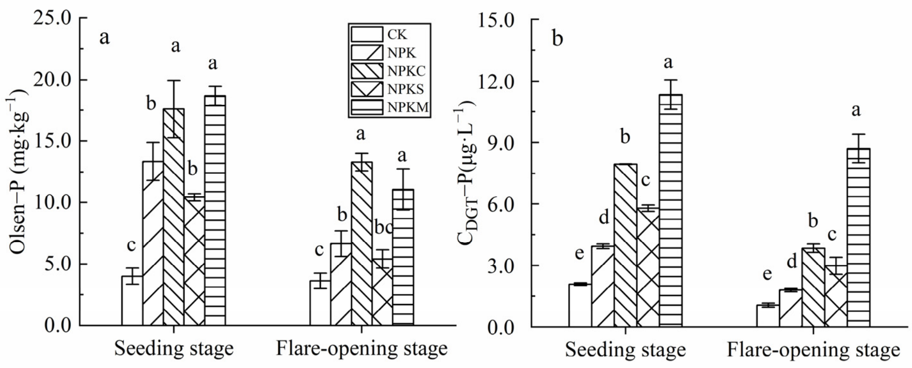

Figure 3. Effects of fertilizer application on Olsen–P (**a**) and C_{DGT}–P (**b**) at the seeding stage and flare–opening stage in the fifth maize season. The different lowercase letters above the bars at the same stage indicate $p < 0.05$.

Table 3. Relationship between maize plant P and soil labile P using Pearson's correlation analysis in fertilized soils.

Soil Labile P	**Plant P**			
	Seeding Stage		**Flare–Opening Stage**	
	Content	**Accumulation**	**Content**	**Accumulation**
Olsen–P	0.713 **	0.195	0.468	0.503
C_{DGT}–P	0.960 **	0.666 *	0.881 **	0.923 **

"*" and "**" represent $p < 0.05$ and $p < 0.01$, respectively.

3.2. Changes in Soil P Fractions during the Fifth Maize Season after Five–Year Fertilization

The contents of soil inorganic Ca_2–P, Ca_8–P, Al–P and Fe–P and organic P (OP) showed significant differences between the treatments (Table 4). A distinct difference in P fractions was not observed among fertilized treatments at the mature stage but was observed at the seeding stage and flare–opening stage. At the seeding stage and flare–opening stage, the contents of the P fractions were ranked as Fe–P < OP < Al–P < Ca_2–P and Ca_8–P under fertilized treatments. Compared to the NPK treatment, the NPKC and NPKM treatments obviously induced higher Ca_2–P by 34.35–200.37%, Ca_8–P by 93.18–328.66%, Al–P by 23.08–151.20% and OP by 91.41–45.83% at the seeding stage and flare–opening stage, and their Fe–P contents increased by 33.29–44.74% at the flare–opening stage. Furthermore, the difference between them at the flare–opening stage was greater than that at the seeding stage. While the NPKS treatment exhibited an advantage only in terms of the OP content by 61.04% at the seeding stage, the inorganic P fractions had no increase relative to the NPK treatment.

The P fractions under fertilized treatments had distinct differences among various maize growth stages (Table 4). As the maize stages progressed, the great P decrease was mainly in the form of inorganic P. From the seeding stage to the flare–opening stage, all fertilization treatments had a similar decrement in Ca_2–P, but Ca_8–P had an obvious increase in the NPKC and NPKM treatments; the NPK and NPKS treatments had a great decrease in Fe–P along with Al–P, which was greater than that in the NPKC and NPKM treatments. For the NPKM treatment, Al–P served as the main source of P decrease over this period. From the flare–opening stage to the mature stage, a substantial decrease in Fe–P, along with Al–P, was observed in the NPKC and NPKM treatments. A minority of the remaining P comprised the P depletion in the NPK and NPKS treatment. Notably, OP tended to significantly increase in the NPK treatment with maize growth, revealing the existence of an OP synthesis mechanism. A significant decrease in OP was observed in the NPKC treatment before the flare–opening stage but occurred in the NPKM treatment after the flare–opening stage.

Table 4. Effects of fertilizer application on soil P fractions during the fifth maize season (mg·kg^{-1}).

Stages	Treatment	Ca_2–P	Ca_8–P	Al–P	Fe–P	OP
Seeding stage	CK	2.40 ± 0.29 Ad	0.42 ± 0.04 Ac	9.02 ± 0.19 Ad	71.66 ± 6.28 Ab	81.81 ± 7.20 Ac
	NPK	15.19 ± 1.94 Ac	3.26 ± 0.23 Ab	42.38 ± 3.64 Ac	167.36 ± 11.10 Aa	74.46 ± 4.83 Cc
	NPKC	20.41 ± 2.88 Ab	6.43 ± 1.09 Aa	52.17 ± 6.51 Ab	184.8 ± 9.49 Aa	142.53 ± 9.79 Aa
	NPKS	16.77 ± 1.12 Ac	4.12 ± 0.18 Ab	42.97 ± 4.46 Ac	161.16 ± 16.57 Aa	102.59 ± 5.99 Ab
	NPKM	25.10 ± 0.65 Aa	6.69 ± 1.00 Ba	71.69 ± 2.87 Aa	180.35 ± 7.76 Aa	127.51 ± 4.39 Aa
Flare–opening stage	CK	1.18 ± 0.19 Ac	0.60 ± 0.09 Ad	7.80 ± 0.63 Ac	66.81 ± 6.51 Bc	78.3 ± 1.46 Ad
	NPK	2.80 ± 0.12 Bc	2.21 ± 0.11 Bc	18.77 ± 0.63 Bb	117.11 ± 9.21 Bb	92.04 ± 2.54 Bcd
	NPKC	6.29 ± 0.50 Bb	7.28 ± 0.21 Ab	39.17 ± 2.20 Ba	163.71 ± 9.07 Ba	115.69 ± 4.92 Bb
	NPKS	1.93 ± 0.27 Bc	1.25 ± 0.17 Bcd	14.16 ± 0.93 Bb	105.27 ± 1.60 Bb	96.51 ± 7.20 Ac
	NPKM	9.46 ± 1.22 Ba	9.46 ± 1.18 Aa	40.92 ± 3.25 Ba	177.77 ± 15.13 Aa	134.22 ± 9.15 Aa
Mature stage	CK	0.35 ± 0.05 Ab	0.01 ± 0.01 Ab	5.59 ± 0.57 Ab	63.88 ± 2.20 Bc	85.65 ± 2.41 Ab
	NPK	2.14 ± 0.23 Ba	1.13 ± 0.06 Ca	13.78 ± 1.48 Ba	86.99 ± 3.88 Ca	110.89 ± 6.24 Aa
	NPKC	3.47 ± 0.32 Ca	1.2 ± 0.34 Ba	17.51 ± 0.10 Ca	101.12 ± 6.90 Ca	105.46 ± 10.01 Ba
	NPKS	2.47 ± 0.28 Ba	1.02 ± 0.11 Ba	18.29 ± 1.89 Ba	99.30 ± 1.42 Ba	113.77 ± 5.78 Aa
	NPKM	3.17 ± 0.43 Ca	0.91 ± 0.04 Ca	15.32 ± 2.52 Ca	95.24 ± 7.17 Ba	105.78 ± 4.43 Ba

Ca_{10}–P and O–P fractions (total 90–143.81 mg·kg^{-1}) were not showed in table due to few changes in maize growth. CK: no fertilizer; NPK: chemical fertilizer; NPKC: chemical fertilizer and bone meal fertilizer; NPKS: chemical fertilizer and crop straw; NPKM: chemical fertilizer and bioorganic fertilizer. The values are the mean ± SD. Different lowercase letters listed in a column at the same stage indicate significant differences at $p < 0.05$ between treatments. Different uppercase letters listed in a column at the same treatment indicate significant differences at $p < 0.05$ between stages.

3.3. Relationships among the Soil Properties, P Fractions and Olsen–P

The RDA plot showed that the RDA1 and RDA2 axes accounted for 77.28% and 10.42% of the total variation in the soil P fractions, respectively (Figure 4a). The results revealed that SOM was the main factor that influenced the P fractions, accounting for 58.9% of the variation, followed by Fe_{pp}, accounting for 17.2% ($p < 0.002$). The pH made a small contribution to the variation, but it was strongly related to the decrease in Fe–P and Al–P with maize growth ($p < 0.01$, Table S1).

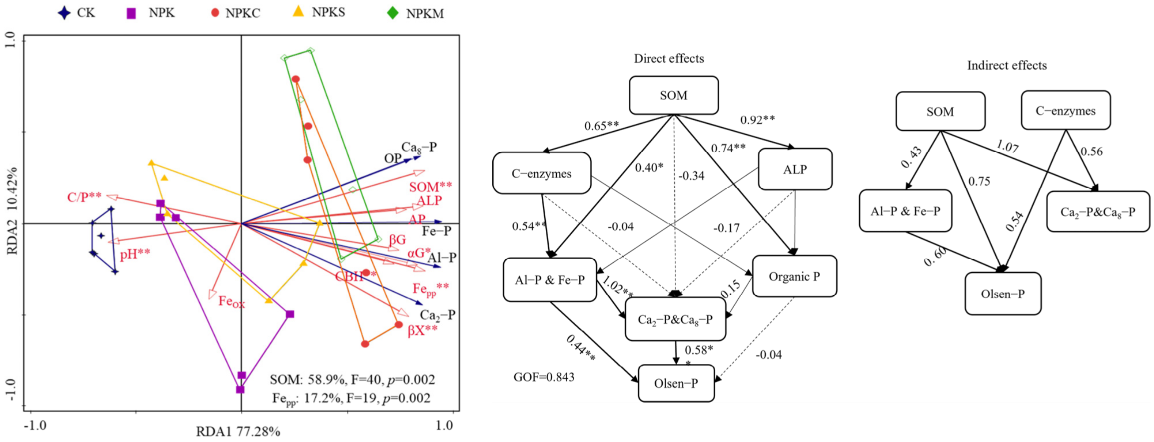

(**a**) (**b**)

Figure 4. Redundancy analysis plots of the correlations between the soil properties and the phosphorus fractions (**a**); the partial least squares path model (PLS–PM) of the direct and indirect effects among the soil SOM, C recycling enzymes, alkaline phosphatase, P fractions and Olsen–P (**b**). The observed variables are shown in the solid boxes. The numbers next to the single–headed arrows are the standardized path coefficients. The black solid and dashed line arrows represent positive and negative correlations, respectively. The goodness of fit (GOF) value is calculated to evaluate the model. "*" indicates $p < 0.05$ and "**" indicates $p < 0.01$.

PLS–PM analysis further showed that the relationships among the soil properties, P fractions and Olsen–P (Figure 4b). SOM had an influence on OP, but OP failed to favor the Olsen–P level. The similar direct and indirect effects (0.40) of SOM were exerted on Al–P and Fe–P, and the indirect effects were realized via C enzymes rather than ALP. A strong effect (1.07) of SOM on Ca_2–P and Ca_8–P was only indirectly via Al–P and Fe–P. Additionally, Ca_2–P and Ca_8–P had significant direct effects on Olsen–P (0.58), while the Al–P and Fe–P fractions had both strong direct (0.44) and indirect effects (0.60) on Olsen–P via Ca_2–P and Ca_8–P, indicating their high supply potential for plants. This indicated that the SOM regulated Olsen–P mainly by influencing Al–P and Fe–P.

3.4. Soil P Resupply Capacity during the Fifth Maize Season after Five–Year Fertilization

Based on the DGT and DIFS simulations, the results showed that fertilization had remarkable effects on the labile P resupply during the fifth maize season (Table 5). For the fertilization treatments, the relatively high R values of 0.31–0.61 and C_E/C_{soln} values of 7.98–15.24 indicated that P resupply played an important role in P mobility. The larger R, C_E and C_E/C_{soln} values in the NPKM, NPKC and NPKS treatments demonstrated their higher resupply capacity compared to those in NPK treatment. Moreover, although the R, C_E and C_E/C_{soln} values decreased at the flare–opening stage, the values under the NPKM treatment remained equal to those under the NPK treatment at the seeding stage. With similar K_d values of 1000 $cm^3 \cdot g^{-1}$ in the fertilized soils at the seeding stage, the NPK treatment had the highest T_c value of 1214 s, while the NPKM treatment had the lowest T_c value of 61 s. By the flare–opening stage, T_c increased to 1049–9403 s and K_d decreased to 407–874 $cm^3 \cdot g^{-1}$ in the fertilized soils. Additionally, Pearson analysis showed that R was highly related to C_E, C_E/C_{soln}, T_c and K_d, and R, C_E, C_E/C_{soln}, and T_c had high correlations with Olsen–P, SOM and Fe_{pp} ($p < 0.05$, Figure 5). The soil pH and Fe_{ox} exerted positive effects on T_c ($p < 0.01$), but they had no significant correlation with R ($p > 0.05$).

Table 5. Kinetic parameters of soil P release based on DGT and DIFS models in soils during the fifth maize season.

Stage	Treatment	R	K_d	T_c	k_1	k_{-1}	R_{diff}	C_E	C_E/C_{soln}
–	–	–	$cm^3 \cdot g^{-1}$	s	s^{-1}	s^{-1}	–	$\mu g \cdot L^{-1}$	–
Seeding stage	CK	0.19	380	4418	2.26×10^{-4}	2.70×10^{-7}	3.86×10^{-2}	53.98	5.01
	NPK	0.31	1080	1214	8.23×10^{-4}	3.59×10^{-7}	3.94×10^{-2}	99.95	7.98
	NPKC	0.47	1060	312	3.20×10^{-3}	1.46×10^{-6}	4.01×10^{-2}	198.12	11.62
	NPKS	0.47	970	290	3.45×10^{-3}	1.70×10^{-6}	3.97×10^{-2}	145.72	11.85
	NPKM	0.61	1000	61	1.64×10^{-2}	8.01×10^{-6}	3.97×10^{-2}	285.56	15.24
Flare–opening stage	CK	0.11	390	17,770	0.56×10^{-4}	6.59×10^{-8}	3.86×10^{-2}	27.59	2.88
	NPK	0.15	591	9403	1.06×10^{-4}	8.50×10^{-8}	3.94×10^{-2}	45.43	3.81
	NPKC	0.25	874	2512	3.51×10^{-4}	2.00×10^{-7}	4.01×10^{-2}	95.95	6.31
	NPKS	0.22	407	3473	3.98×10^{-4}	2.21×10^{-7}	3.96×10^{-2}	75.32	5.51
	NPKM	0.33	431	1049	9.52×10^{-4}	1.08×10^{-6}	3.97×10^{-2}	219.15	8.28

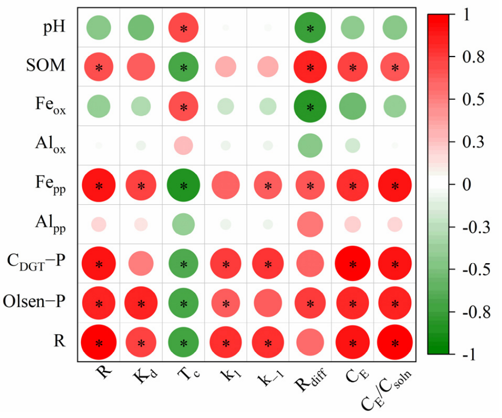

Figure 5. Pearson correlation analysis of the P kinetic resupply parameters and soil properties during the fifth maize season. "*" indicates $p < 0.05$.

3.5. PLS–PM among the Soil Properties, P Supply Pools, P Resupply and Plant P Uptake

The PLS–PM was used to explore the correlations among the soil properties, P supply pools, P resupply and plant P uptake (Figure 6). The results indicated that plant P uptake was directly affected by P resupply (0.72) and was indirectly affected by P supply pools (0.83). SOM and Fe_{pp} directly affected P supply pools (0.79) to mediate P resupply (1.09) and plant P uptake (0.62). The significant effect of SOM and Fe_{pp} on the C enzymes (0.83) and ALP activities (0.86) failed to contribute to P supply pools and plant P uptake. Additionally, the high loading values (0.83–0.97) of inorganic P (Ca_2–P, Ca_8–P, Al–P and Fe–P) revealed that they played a crucial role in the P supply pool, while the low loading value (0.36) of OP revealed that OP slightly contributed to the P supply pool for plant uptake.

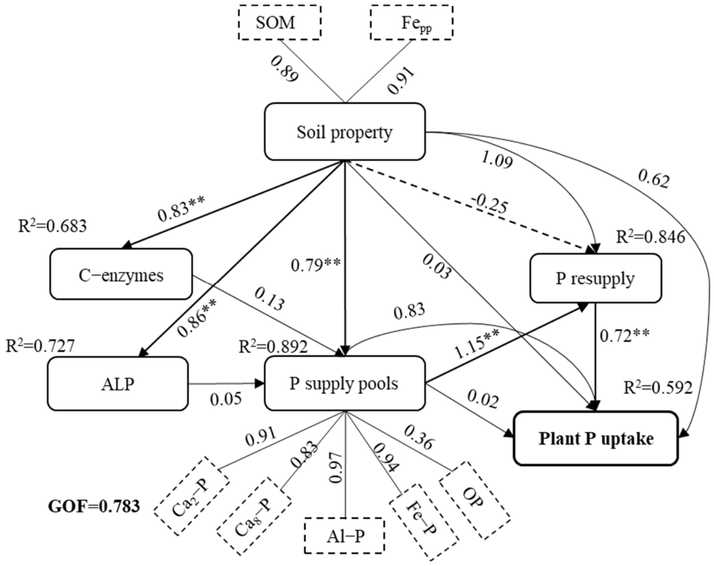

Figure 6. Partial least squares path model (PLS–PM) of the direct and indirect effects of the soil properties, C recycling enzymes, phosphatase and P fractions on plant P uptake. The observed variables are shown in the solid boxes. The numbers next to the single–headed arrows are the standardized path coefficients. The black solid and dashed line arrows represent negative and positive correlations, respectively. The value between the bold solid boxes is the correlation coefficient. The dotted boxes are the loadings of the latent variables. The goodness of fit (GOF) value is calculated to evaluate the model. "**" indicates $p < 0.01$.

4. Discussion

4.1. The Soil P Fractions and P Availability to Plants after Fertilization

The characteristics of the P fractions and P availability in soils provide a better understanding of the dynamic changes in the P supply pool for plants. Present studies indicate that the NPKC and NPKM treatments had significantly higher OP and inorganic Ca_2–P, Ca_8–P and Al–P fractions early in the fifth maize season compared to NPK treatment (Table 4). The distinct P fractions and P forms in many organic fertilizers has been reported to directly affect the soil P fractions when repeatedly applied to soils [4,44]. Coincidently, the higher organic fertilizer–P input was observed only in NPKC and NPKM treatments (Tables 1 and 4). Straw with relatively low P had a long–term decomposition process, providing a lagged limited release of nutrients in soils [45,46]. Additionally, SOM played a crucial role in the transformation of P fractions under organic fertilization [13], which agreed with our result that SOM positively affected the OP and inorganic P fractions (Figure 4). As OP is the compound mostly containing C–O–P bonds, the OP content is usually associated with SOM accumulation [13,47]. Previous studies found that soil organic acids (important components of SOM) directly reduced the P binding sites and increased available P contents by chemical reactions, including competitive adsorption, metal complexation and dissolution reactions [44,48]. A notable finding of our study was that the SOM accumulation directly and indirectly favored Al–P and Fe–P retention (Figure 4b). Although little direct evidence explained the relationship, it was reported that some specific OM compounds (such as humic) favored the existence of OM–Fe/Al–P–complexes as colloids [48]. The clear association of the OM compositions with the P fractions, especially Al–P and Fe–P, should be further investigated in the future.

OP, as an important part of soil P, can be mineralized into labile inorganic P for plant uptake, which is mainly dominated by extracellular phosphatase (AC and ALP) [49,50]. Long–term organic fertilizer addition was usually reported to promoted OP mineralization reflected by the decrease of OP [51,52]. An increase of OP occurred in the NPK treatment (Table 4), which was attributed to the superiority of microbial labile P immobilization over OP mineralization [4]. The significant decrease of OP in the NPKC and NPKM treatments and the higher ALP activity coincidently suggested the OP mineralization (Figure S2 and Table 4). Nerveless, a negligible effect of ALP and OP on Olsen–P (Figure 4) indicated that OP failed to contribute to the available P by mentalization in our study. This might occur because the inorganic P by OP mineralization might be limited in the short–term maize growth. Guo et al. [53] also reported that OP made no significant contribution to the available P when receiving high inorganic P levels under intensive plant growth. Further trials are needed to find which specific OP fractions contribute to P uptake.

P fertilization enriched the inorganic P pool to a great extent (Table 4), especially the Al–P and Fe–P fractions, which are the main inorganic P fractions in acidic soils [54]. Ca_2–P was the effective source of P for crop growth, and Ca_8–P, Al–P and Fe–P were less available P fractions in calcareous soils [39]. Ca_8–P, along with Ca_2–P, had an obvious direct effect on Olsen–P (Figure 4), suggesting that they serve as available P for plants in acidic soil. Significant direct and indirect effects of the Al–P and Fe–P fractions on Olsen–P indicated their high supply potential to available P (Figure 4), which is consistent with the report by Chen et al. [54]. The great decrease of Fe/Al–P with maize growth related to pH was observed in this study (Table 4 and Table S1), which further confirmed the contribution of Fe/Al–P to available P for plant. When the pH decreased due to the secretion of protons and organic anions, the dissolution of Fe–P, Al–P and Ca–P in soils was stimulated to enhance dissolved P [3,55]. The application of alkaline organic fertilizers in NPKC and NPKM treatments buffered the decrease in pH and delayed the Fe–P release until a late stage (Table 4 and Figure S1), where great P was demanded by maize growth for better plant P uptake, which not only satisfied the P requirement rules for maize growth, but also promoted P fertilizer utilization efficiency.

Additionally, many reports showed that long–term fertilization contributed to P buildup, and culminated in the saturation of P sorption sites, resulting in a high level of available P which was easily released into the soil solution and finally increased the potential of P loss by runoff or leaching [54,56,57]. After a five–year application, the total P accumulation was below 400 $mg \cdot kg^{-1}$, and the available P fractions at a mature stage was less than 5 $mg \cdot kg^{-1}$ (Table 4). The concentration of Olsen–P is often used as an indicator to determine the P leaching risk [7,56]. Pradhan et al. [7] reported the change–point Olsen P at 50.4 $mg \cdot kg^{-1}$ for clay loam soils. Li et al. [56] summarized that the critical level of Olsen–P in the topsoil for production of maize is 28.20 $mg \cdot kg^{-1}$, and 78.2 $mg \cdot kg^{-1}$ for the P leaching potential in South China. In contrast, after five–year fertilization, even though the fresh fertilizers were lately applied in season, the Olsen–P contents were 25 $mg \cdot kg^{-1}$ at most at the seeding stage in our fertilized soils (Figure 3), which was far less than the above critical Olsen–P contents for loss. This suggests that our repeated application of combined inorganic and organic fertilizers favored the P supply for plants and can also continue to be ploughed into soils for years. This indicates that our organic fertilization practices can be developed for sustainable repeated management practices in agriculture production.

4.2. The Dynamic P Resupply to Plants after Fertilization

The C_{DGT}–P and C_E concentration represented the labile P effective mobility for plant. The R value ($\leq$1) and C_E/C_{soln} ratio (>1) separately reflected the resupply capacity and the contribution of labile P in soil solids to P mobility for plants [58]. High C_E values of over 1000 $\mu g \cdot L^{-1}$ but relatively low R (0.1–0.2) and C_E/C_{soln} values (1.5–3.0) were observed in many heavily fertilized soils [28]. This might suggest that in high–P soils, solution P is most likely enough for P mobility, which slightly induced a labile P resupply from solids. In contrast, the C_E values of 99.95–285.56 $\mu g \cdot L^{-1}$ along with relatively high R (0.31–0.60) and C_E/C_{soln} (7.98–15.24) values were detected at an early stage of plant growth in our fertilized soils (Table 5), which was in accordance with other studies in acidic soils [59]. This highlighted the fact that the labile P resupply played a crucial role in P mobility in low–P soils.

K_d and T_c are considered to limit long– and short–term R, respectively. Relatively large T_c values of 1×10^3–1×10^5 s were always tied with relatively low K_d (<200 $cm^3 \cdot g^{-1}$) values in some soils [29,60]. The T_c values of 61–9403 s accompanied with K_d values of 407–1000 $cm^3 \cdot g^{-1}$ were observed in our fertilized soils (Table 5). Moreover, compared to those in the NPK treatment, the larger R, C_E, C_E/C_{soln} and lower T_c in the NPKS, NPKC and NPKM treatments indicated that they had a greater P resupply capacity to enhance dissolved P for plant, which was attributed to the acceleration of P release from soil solid. This revealed the reason for the better plant P uptake of NPKS treatment than that of NPK treatment under same level of labile P (Figures 2 and 3). The result suggested that when slight variations in labile P pools or in the P adsorption capacity were induced by organic fertilizers, the DGT method seemed to be more sensitive to the difference in P supply, as observed by Mackay et al. [5] in plant–available P in organic–amended soils.

Ernstberger et al. [61] showed that when $T_c > 10$ s, kinetic release imposed great impacts on P resupply in the short term, but labile pools finally controlled long–term resupply. Menezes–Blackburn et al. [28] also found that the resupply capacity was significantly associated with the P status in 32 soils. Similarly, the available P imposed a great influence on P resupply, and SOM and Fe_{pp} also indirectly regulated P resupply by influencing the P supply pools (Figures 5 and 6). Almås et al. [62] showed that the notable partitioning of rapidly available P resulted in a substantial reduction in T_c in long–term fertilized soils. With a distinct difference in labile P, the equal R and T_c values in the NPKS and NPKC treatments (Figure 3 and Table 5) might suggest that except for labile P, other factors (e.g., soil particle structure) ignored in our study favored the P resupply capacity [28]. Our PMLS–PM results also suggested that P resupply directly dominated plant P uptake, which was also greatly mediated by the inorganic P supply pool (Figure 6). The higher inorganic P supply pools in the NPKC and NPKM treatments favored higher plant P uptake than that in the NPKS treatments, promoting more efficient P utilization.

5. Conclusions

After five–year fertilization, P resupply decisively affected P uptake by maize, which is controlled by the labile P pool and the P release during the fifth maize season. A limited OP mineralization made no contribution to available P for plants. Inorganic Ca_2–P, Ca_8–P, Al–P and Fe–P had a great effect on the available P. The potential contribution of the Fe–P and Al–P effective release stimulated by pH to plant cannot be underestimated in NPKC and NPKM treatments. SOM was the dominant factor that effected the P fractions and P availability, which finally regulated P resupply and plant uptake. Compared to NPK treatment, the NPKS treatment promoted P resupply by accelerating the labile P release to increase plant uptake; the NPKC and NPKM treatments promoted the inorganic available and slow–available P and enhanced P resupply for a better increase in P uptake by maize. Therefore, management practices such as long–term NPKC and NPKM application must be developed during the maize season for high P use efficiency in sustainable agriculture.

Supplementary Materials: The following supporting information can be downloaded at: https://www.mdpi.com/article/10.3390/agriculture13040858/s1, Figure S1: Effects of fertilizer application on (a) SOM and (b) pH at different growth stages. Figure S2: Effects of fertilizer application on soil enzyme activities at different growth stages. Table S1: Relationship between the P decrease and soil properties using Pearson's method. Materials and Method SM 2.1 [63,64].

Author Contributions: Software, J.Z.; preparation, J.W., Z.P. and C.T.; formal analysis, J.Z., J.W. and Z.P.; investigation, J.Z., J.W., C.T. and Z.P.; data curation, Y.W., N.Z. and S.S.; writing—original draft, J.Z., N.Z., Y.W., S.S. and X.Z.; writing—review and editing, J.Z., Y.Z., T.Z., S.S. and X.Z.; Supervision, X.Z.; funding acquisition, X.Z., Y.W. and Y.Z. All authors have read and agreed to the published version of the manuscript.

Funding: This research was funded by the National Natural Science Foundation of China (Grant Nos. U19A2048, 41907088 and 41877061), the National Key R&D Program of China (Grant No. 2021YFD1901201–01) and the Central Public–interest Scientific Institution Basal Research Fund (Grant No. Y2022LM28).

Institutional Review Board Statement: Not applicable.

Data Availability Statement: All the data reported here are available from the authors upon request.

Conflicts of Interest: The authors declare no conflict of interest.

References

1. Cordell, D.; Drangert, J.O.; White, S. The story of phosphorus: Global food security and food for thought. *Glob. Environ. Chang.* **2009**, *19*, 292–305. [CrossRef]
2. Jin, Z.W.; Chen, C.; Chen, X.M.; Jiang, F.; Hopkins, I.; Zhang, X.L.; Han, Z.Q.; Billy, G.; Benavides, J. Soil acidity, available phosphorus content, and optimal biochar and nitrogen fertilizer application rates: A five–year field trial in upland red soil, china. *Field Crop. Res.* **2019**, *232*, 77–87. [CrossRef]
3. Wang, Y.Z.; Chen, X.; Whalen, J.K.; Cao, Y.H.; Quan, Z.; Lu, C.Y.; Shi, Y. Kinetics of inorganic and organic phosphorus release influenced by low molecular weight organic acids in calcareous, neutral and acidic soils. *J. Plant Nutr. Soil Sci.* **2015**, *178*, 555–566. [CrossRef]
4. Zhao, F.Y.; Zhang, Y.Y.; Dijkstra, F.A.; Li, Z.J.; Zhang, Y.Q.; Zhang, T.S.; Lu, Y.Q.; Shi, J.W.; Yang, L.J. Effects of amendments on phosphorous status in soils with different phosphorous levels. *Catena* **2019**, *172*, 97–103. [CrossRef]
5. Mackay, J.E.; Macdonald, L.M.; Smernik, R.J.; Cavagnaro, T.R. Organic amendments as phosphorus fertilisers: Chemical analyses, biological processes and plant p uptake. *Soil. Biol. Biochem.* **2017**, *107*, 50–59. [CrossRef]
6. Abdala, D.B.; da Silva, I.R.; Vergutz, L.; Sparks, D.L. Long–term manure application effects on phosphorus speciation, kinetics and distribution in highly weathered agricultural soils. *Chemosphere* **2015**, *119*, 504–514. [CrossRef]
7. Pradhan, S.N.; Ghosh, A.K.; Seema; Ram, S.; Pal, Y.; Pradhan, C. Changes in degree of phosphorus saturation and risk of p loss upon twelve years of manuring and reduced tillage. *Geoderma* **2021**, *404*, 115277. [CrossRef]
8. Six, L.; Smolders, E.; Merckx, R. The performance of dgt versus conventional soil phosphorus tests in tropical soils—Maize and rice responses to p application. *Plant Soil* **2012**, *366*, 49–66. [CrossRef]
9. Nawara, S.; Van Dael, T.; Merckx, R.; Amery, F.; Elsen, A.; Odeurs, W.; Vandendriessche, H.; Mcgrath, S.; Roisin, C.; Jouany, C.; et al. A comparison of soil tests for available phosphorus in long–term field experiments in europe. *Eur. J. Soil Sci.* **2017**, *68*, 873–885. [CrossRef]
10. Crews, T.E. The supply of phosphorus from native, inorganic phosphorus pools in continuously cultivated mexican agroecosystems. *Agric. Ecosyst. Environ.* **1996**, *57*, 197–208. [CrossRef]
11. Nobile, C.M.; Bravin, M.N.; Becquer, T.; Paillat, J.M. Phosphorus sorption and availability in an andosol after a decade of organic or mineral fertilizer applications: Importance of ph and organic carbon modifications in soil as compared to phosphorus accumulation. *Chemosphere* **2020**, *239*, 124709. [CrossRef]
12. Zhang, Y.; Gao, W.; Luan, H.; Tang, J.; Li, R.; Li, M.; Zhang, H.; Huang, S. Long–term organic substitution management affects soil phosphorus speciation and reduces leaching in greenhouse vegetable production. *J. Clean. Prod.* **2021**, *327*, 129464. [CrossRef]
13. Wei, L.; Chen, S.; Cui, J.; Ping, H.; Yuan, C.; Chen, Q. A meta–analysis of arable soil phosphorus pools response to manure application as influenced by manure types, soil properties, and climate. *J. Environ. Manag.* **2022**, *313*, 115006. [CrossRef]
14. Iqbal, S.M. *Effect of Crop Residue Qualities on Decomposition Rates, Soil Phosphorus Dynamics and Plant Phosphorus Uptake*; The University of Adelaide: Adelaide, Australia, 2009.
15. Jalali, M.; Ranjbar, F. Rates of decomposition and phosphorus release from organic residues related to residue composition. *J. Plant Nutr. Soil Sci.* **2009**, *172*, 353–359. [CrossRef]
16. Alamgir, M.; McNeill, A.; Tang, C.X.; Marschner, P. Changes in soil p pools during legume residue decomposition. *Soil. Biol. Biochem.* **2012**, *49*, 70–77. [CrossRef]
17. Garg, S.; Bahl, G.S. Phosphorus availability to maize as influenced by organic manures and fertilizer p associated phosphatase activity in soils. *Bioresour. Technol.* **2008**, *99*, 5773–5777. [CrossRef]
18. Noack, S.R.; McBeath, T.M.; McLaughlin, M.J.; Smernik, R.J.; Armstrong, R.D. Management of crop residues affects the transfer of phosphorus to plant and soil pools: Results from a dual–labelling experiment. *Soil. Biol. Biochem.* **2014**, *71*, 31–39. [CrossRef]
19. Moody, P.W.; Aitken, R.L.; Compton, B.L.; Hunt, S. Soil phosphorus parameters affecting phosphorus availability to, and fertilizer requirements of, maize (zea mays). *Soil Res.* **1988**, *26*, 611–622. [CrossRef]

20. Ehlert, P.; Morel, C.; Fotyma, M.; Destain, J.P. Potential role of phosphate buffering capacity of soils in fertilizer management strategies fitted to environmental goals. *J. Plant Nutr. Soil Sci.* **2003**, *166*, 409–415. [CrossRef]
21. Blume, H.–P.; Brümmer, G.W.; Horn, R.; Kandeler, E.; Kögel–Knabner, I.; Kretzschmar, R.; Stahr, K.; Wilke, B.–M. *Scheffer/Schachtschabel: Lehrbuch der Bodenkunde*, 3rd ed.; Springer: Berlin/Heidelberg, Germany, 2016.
22. Weihrauch, C.; Opp, C. Ecologically relevant phosphorus pools in soils and their dynamics: The story so far. *Geoderma* **2018**, *325*, 183–194. [CrossRef]
23. Van Rotterdam, A.M.D.; Bussink, D.W.; Temminghoff, E.J.M.; Van Riemsdijk, W.H. Predicting the potential of soils to supply phosphorus by integrating soil chemical processes and standard soil tests. *Geoderma* **2012**, *189–190*, 617–626. [CrossRef]
24. Delgado, A.; del Campillo, M.D.; Torrent, J. Limitations of the olsen method to assess plant–available phosphorus in reclaimed marsh soils. *Soil Use Manag.* **2010**, *26*, 133–140. [CrossRef]
25. Zhang, C.; Ding, S.; Xu, D.; Tang, Y.; Wong, M.H. Bioavailability assessment of phosphorus and metals in soils and sediments: A review of diffusive gradients in thin films (dgt). *Environ. Monit. Assess.* **2014**, *186*, 7367–7378. [CrossRef] [PubMed]
26. Davison, W.; Zhang, H. Progress in understanding the use of diffusive gradients in thin films (dgt)—Back to basics. *Environ. Chem.* **2012**, *9*, 1–13. [CrossRef]
27. Harper, M.P.; Davison, W.; Tych, W. Difs—A modelling and simulation tool for dgt induced trace metal remobilisation in sediments and soils. *Environ. Model. Softw.* **2000**, *15*, 55–66. [CrossRef]
28. Menezes–Blackburn, D.; Zhang, H.; Stutter, M.; Giles, C.D.; Darch, T.; George, T.S.; Shand, C.; Lumsdon, D.; Blackwell, M.; Wearing, C.; et al. A holistic approach to understanding the desorption of phosphorus in soils. *Environ. Sci. Technol.* **2016**, *50*, 3371–3381. [CrossRef]
29. Kalkhajeh, Y.K.; Sorensen, H.; Huang, B.; Guan, D.X.; Luo, J.; Hu, W.; Holm, P.E.; Hansen, H.C.B. Dgt technique to assess p mobilization from greenhouse vegetable soils in china: A novel approach. *Sci. Total Environ.* **2018**, *630*, 331–339. [CrossRef]
30. FAO/IUSS. *World Reference Base for Soil Resources*; FAO: Rome, Italy, 2015.
31. Komy, Z.R. Comparative–study of titrimetric and gravimetric methods for the determination of organic–carbon in soils. *Int. J. Environ. Anal. Chem.* **1995**, *60*, 41–47. [CrossRef]
32. Minasny, B.; McBratney, A.B.; Wadoux, A.M.J.C.; Akoeb, E.N.; Sabrina, T. Precocious 19th century soil carbon science. *Geoderma Reg.* **2020**, *22*, e00306. [CrossRef]
33. Guibal, R.; Buzier, R.; Lissalde, S.; Guibaud, G. Adaptation of diffusive gradients in thin films technique to sample organic pollutants in the environment: An overview of o–dgt passive samplers. *Sci. Total Environ.* **2019**, *693*, 133537. [CrossRef]
34. Romanya, J.; Blanco–Moreno, J.M.; Sans, F.X. Phosphorus mobilization in low–p arable soils may involve soil organic c depletion. *Soil Biol. Biochem.* **2017**, *113*, 250–259. [CrossRef]
35. Olsen, S.R. Estimation of Available Phosphorus in Soils by Extraction with Sodium Bicarbonate. 1954. Available online: https://agris.fao.org/agris$-$search/search.do?recordID=US201300436954 (accessed on 10 May 2020).
36. Wolf, B. A comprehensive system of leaf analyses and its use for diagnosing crop nutrient status. *Commun. Soil Sci. Plant Anal.* **2008**, *13*, 1035–1059. [CrossRef]
37. Murphy, J.; Riley, J.P. A modified single solution method for the determination of phosphate in natural waters. *Anal. Chim. Acta* **1962**, *27*, 31–36. [CrossRef]
38. Saiya–Cork, K.R.; Sinsabaugh, R.L.; Zak, D.R. The effects of long term nitrogen deposition on extracellular enzyme activity in an acer saccharum forest soil. *Soil Biol. Biochem.* **2002**, *34*, 1309–1315. [CrossRef]
39. Jiang, B.; Gu, Y. A suggested fractionation scheme of inorganic phosphorus in calcareous soils. *Fertil. Res.* **1989**, *20*, 159–165. [CrossRef]
40. Ding, S.; Xu, D.; Sun, Q.; Yin, H.; Zhang, C. Measurement of dissolved reactive phosphorus using the diffusive gradients in thin films technique with a high–capacity binding phase. *Environ. Sci. Technol.* **2010**, *44*, 8169–8174. [CrossRef]
41. Van Veldhoven, P.P.; Mannaerts, G.P. Inorganic and organic phosphate measurements in the nanomolar range. *Anal. Biochem.* **1987**, *161*, 45–48. [CrossRef]
42. Zhang, H.; Davison, W. Use of diffusive gradients in thin–films for studies of chemical speciation and bioavailability. *Environ. Chem.* **2015**, *12*, 85–101. [CrossRef]
43. Sochaczewski, L.; Tych, W.; Davison, B.; Zhang, H. 2d dgt induced fluxes in sediments and soils (2d difs). *Environ. Model. Softw.* **2007**, *22*, 14–23. [CrossRef]
44. Urrutia, O.; Guardado, I.; Erro, J.; Mandado, M.; Garcia–Mina, J.M. Theoretical chemical characterization of phosphate–metal–humic complexes and relationships with their effects on both phosphorus soil fixation and phosphorus availability for plants. *J. Sci. Food Agric.* **2013**, *93*, 293–303. [CrossRef]
45. Guan, X.K.; Wei, L.; Turner, N.C.; Ma, S.C.; Yang, M.D.; Wang, T.C. Improved straw management practices promote in situ straw decomposition and nutrient release, and increase crop production. *J. Clean. Prod.* **2020**, *250*, 119514. [CrossRef]
46. Huang, T.T.; Yang, N.; Lu, C.; Qin, X.L.; Siddique, K.H.M. Soil organic carbon, total nitrogen, available nutrients, and yield under different straw returning methods. *Soil Tillage Res.* **2021**, *214*, 105171. [CrossRef]
47. Keller, M.; Oberson, A.; Annaheim, K.E.; Tamburini, F.; Mäder, P.; Mayer, J.; Frossard, E.; Bünemann, E.K. Phosphorus forms and enzymatic hydrolyzability of organic phosphorus in soils after 30 years of organic and conventional farming. *J. Plant Nutr. Soil Sci.* **2012**, *175*, 385–393. [CrossRef]

48. Guppy, C.N.; Menzies, N.W.; Moody, P.W.; Blamey, F.P.C. Competitive sorption reactions between phosphorus and organic matter in soil: A review. *Aust. J. Soil Res.* **2005**, *43*, 189–202. [CrossRef]
49. Li, J.; Xie, T.; Zhu, H.; Zhou, J.; Li, C.; Xiong, W.; Xu, L.; Wu, Y.; He, Z.; Li, X. Alkaline phosphatase activity mediates soil organic phosphorus mineralization in a subalpine forest ecosystem. *Geoderma* **2021**, *404*, 115376. [CrossRef]
50. Kwabiah, A.B.; Stoskopf, N.C.; Palm, C.A.; Voroney, R.P.; Rao, M.R.; Gacheru, E. Phosphorus availability and maize response to organic and inorganic fertilizer inputs in a short term study in western kenya. *Agric. Ecosyst. Environ.* **2003**, *95*, 49–59. [CrossRef]
51. Annaheim, K.E.; Doolette, A.L.; Smernik, R.J.; Mayer, J.; Oberson, A.; Frossard, E.; Bünemann, E.K. Long–term addition of organic fertilizers has little effect on soil organic phosphorus as characterized by 31p nmr spectroscopy and enzyme additions. *Geoderma* **2015**, *257–258*, 67–77. [CrossRef]
52. Ahlgren, J.; Djodjic, F.; Börjesson, G.; Mattsson, L. Identification and quantification of organic phosphorus forms in soils from fertility experiments. *Soil Use Manag.* **2013**, *29*, 24–35. [CrossRef]
53. Guo, F.; Yost, R.S.; Hue, N.V.; Evensen, C.I.; Silva, J.A. Changes in phosphorus fractions in soils under intensive plant growth. *Soil Sci. Soc. Am. J.* **2000**, *64*, 1681–1689. [CrossRef]
54. Chen, X.; Yan, X.; Wang, M.; Cai, Y.; Weng, X.; Su, D.; Guo, J.; Wang, W.; Hou, Y.; Ye, D.; et al. Long–term excessive phosphorus fertilization alters soil phosphorus fractions in the acidic soil of pomelo orchards. *Soil Tillage Res.* **2022**, *215*, 105214. [CrossRef]
55. Sun, B.; Gao, Y.; Wu, X.; Ma, H.; Zheng, C.; Wang, X.; Zhang, H.; Li, Z.; Yang, H. The relative contributions of ph, organic anions, and phosphatase to rhizosphere soil phosphorus mobilization and crop phosphorus uptake in maize/alfalfa polyculture. *Plant Soil* **2019**, *447*, 117–133. [CrossRef]
56. Li, H.; Liu, J.; Li, G.; Shen, J.; Bergstrom, L.; Zhang, F. Past, present, and future use of phosphorus in chinese agriculture and its influence on phosphorus losses. *Ambio* **2015**, *44* (Suppl. 2), S274–S285. [CrossRef]
57. Pizzeghello, D.; Berti, A.; Nardi, S.; Morari, F. Relationship between soil test phosphorus and phosphorus release to solution in three soils after long–term mineral and manure application. *Agric. Ecosyst. Environ.* **2016**, *233*, 214–223. [CrossRef]
58. Xu, Q.; Gao, L.; Peng, W.; Gao, B.; Xu, D.; Sun, K. Assessment of labile zn in reservoir riparian soils using dgt, difs, and sequential extraction. *Ecotoxicol. Environ. Saf.* **2018**, *160*, 184–190. [CrossRef]
59. Hong, C.; Su, Y.; Lu, S. Phosphorus availability changes in acidic soils amended with biochar, fly ash, and lime determined by diffusive gradients in thin films (dgt) technique. *Environ. Sci. Pollut. Res.* **2018**, *25*, 30547–30556. [CrossRef]
60. Heidari, S.; Reyhanitabar, A.; Oustan, S. Kinetics of phosphorus desorption from calcareous soils using dgt technique. *Geoderma* **2017**, *305*, 275–280. [CrossRef]
61. Ernstberger, H.; Davison, W.; Zhang, H.; Tye, A.; Young, S. Measurement and dynamic modeling of trace metal mobilization in soils using dgt and difs. *Environ. Sci. Technol.* **2002**, *36*, 349–354. [CrossRef]
62. Almås, Å.R.; Sævarsson, H.T.; Krogstad, T. The partitioning of p in soil determines the fluxes and deliveries of labile p in soil solution. *Geoderma* **2017**, *306*, 135–143. [CrossRef]
63. Thomas, R.L.; Sheard, R.W.; Moyer, J.R. Comparison of conventional and automated procedures for nitrogen, phosphorus, and potassium analysis of plant material using a single digestion. *Agron. J.* **1967**, *59*, 240–243. [CrossRef]
64. Lu, R.K. *Analysis Method of Soil Agricultural Chemistry*; China Agricultural Science and Technology: Beijing, China, 2000.